UCRL-JC-127545
PREPRINT

# Chemical Bonding in Hard Boron-Nitride Multilayers

Alan F. Jankowski
Jeffrey P. Hayes

This paper was prepared for submittal to the
Diamond and Related Materials Journal
and
Diamond 1997
Edinburgh, Scotland
August 3-8, 1997

June 1997

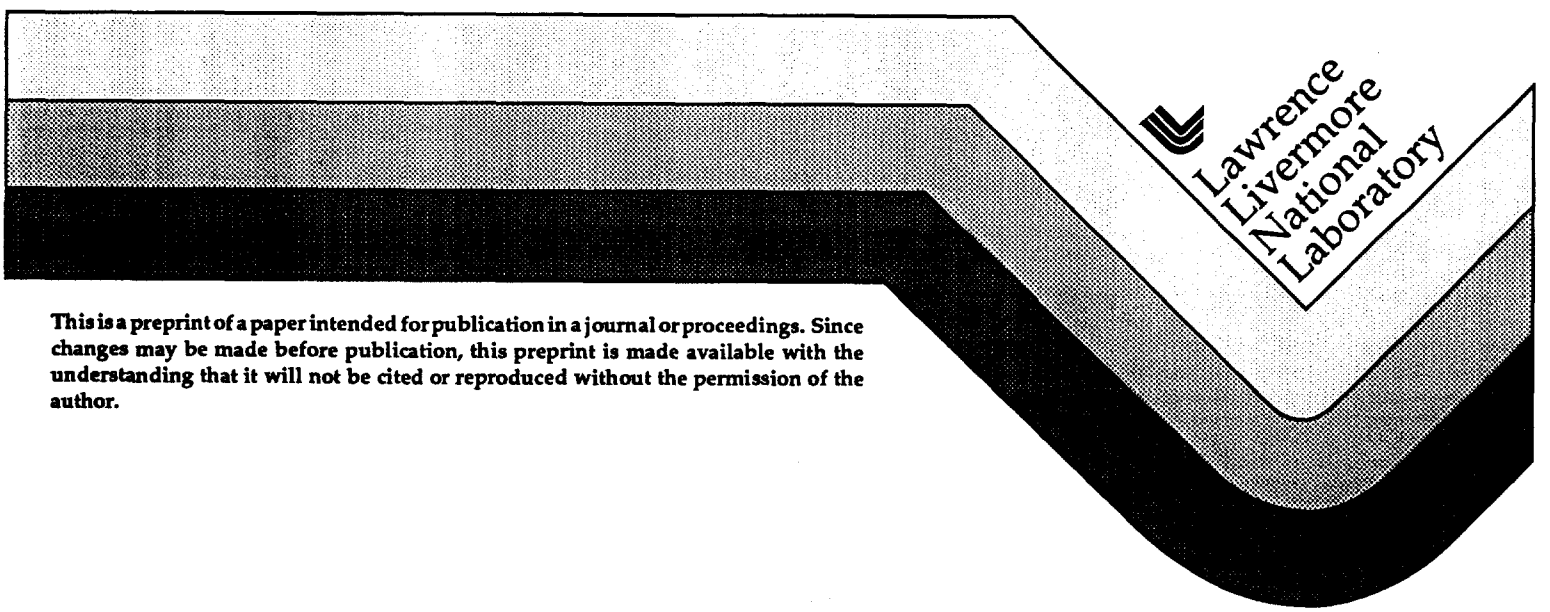

# CHEMICAL BONDING IN HARD BORON-NITRIDE MULTILAYERS

**Alan F. Jankowski and Jeffrey P. Hayes**

University of California - Lawrence Livermore National Laboratory
Department of Chemistry & Materials Science, Livermore, CA 94550 USA

## ABSTRACT

The oxides and nitrides of boron show great potential for use as hard, wear resistant materials. However, large intrinsic stresses and poor adhesion often accompany the hard coatings as found for the cubic boron-nitride phase. These effects may be moderated through the use of a layered structure. Alternate stiff layers of boron (B) and compliant layers of boron-nitride (BN) are formed by modulating the sputter gas composition during deposition from a pure B target. The B/BN thin films are characterized with transmission electron microscopy to evaluate the microstructure, nanoindentation to measure hardness and x-ray absorption spectroscopy to determine chemical bonding. The effects of layer pair spacing on chemical bonding and hardness are evaluated for the B/BN films.

## INTRODUCTION

Vapor deposition techniques have been developed to apply coatings of pure boron (B) and boron nitride (BN) for utilization of their electrical and mechanical properties. The hard, cubic phase of BN has been routinely formed through very energetic deposition processes.[1-4] The application of high voltage, bias sputtering or ion beam bombardment at the substrate is typical and often produces large residual stresses within the coatings. Therefore, if possible, it would be desireable to form the hard coatings through a less eneregetic process. In an alternative approach, a B-based multilayered structure may take advantage of the high hardness property without the formation of large residual stresses.[5] Multilayering, i.e. composition modulating, a thin film inhibits dislocation mobility.[6,7] The multilayer strength and hardness should increase as the modulation wavelength $\lambda$ decreases sufficiently to cease dislocation generation mechanisms within a given layer.

A technique to measure the hardness $H$ of protective multilayer coatings is nanoindentation. Measurement of the hardness of submicron thick coatings requires control of

indentation depths to less than 10 nm.[8,9] There are many examples of hardness enhancement in multilayer and strained layered superlattice coatings. A 75% increase in the microhardness was measured for single crystal TiN/VN(100) superlattices prepared by reactive magnetron sputtering for $\lambda$ decreasing from 32 to 7.5 nm.[10] The hardness increased an additional 75% as the $\lambda$ further decreased to 5 nm, below which the hardness decreased to a rule-of-mixtures (r-o-m) value. In a second example, the hardness of $(TiN)_{0.7}/(NiCr)_{0.3}$ multilayers sputter deposited onto tool steels were assessed using an indentation penetration depth that was less than 10% of the film thickness.[11] The coating hardness increased to a maximum that was 60% above the r-o-m value as $\lambda$ decreased to 1.2 nm. Hardness enhancement in multilayers is not always large as large as for strained layered superlattices.[12] For example, only a 10% increase in hardness is found for Cu/Cr laminates.[13] Although the B/BN multilayers are not anticipated to form a superlattice, the use of nanometric $\lambda(s)$ may create a hardness that exceeds the r-o-m value in an adherent coating.

## EXPERIMENTS AND RESULTS

### *Synthesis Method*

The development of B sputter targets has facilitated the investigation of B and BN deposition without the presence of BN precursor compounds as the hexagonal phase.[14-16] Films of B and BN deposited at low temperature are prepared to establish the baseline properties of the multilayer structures which will consist of a hard B layer alternating with a compliant BN layer. In these experiments, the (hexagonal) BN layer is intended to moderate residual stresses formed within the coating by the hard layer. The deposition of the B coating proceeds by rf-sputtering the B target using an unbalanced planar magnetron.[15-17] The deposition chamber is cryogenically pumped to a base pressure of $5.3 \times 10^{-6}$ Pa in 12 hrs including a 4 hr, 100 °C bake out. Sapphire wafers and 20-50nm thick Ni-coatings on Si wafers (Ni/Si) are used as the substrates which are horizontally positioned 9 cm away from the center of the 6.4cm diameter B target. The sapphire wafers are heated to 450 °C and the Ni/Si wafers are heated to 215 °C using a Boralectric™ heater. The sputter gas pressure is nominally selected as 1 Pa (7 mTorr) with a constant flow rate of 28 cc/min. The deposition rate is monitored with a calibrated 6 MHz Au-coated quartz crystal. An increase in forward power from 100 to 300 W produces a linear increase in deposition rate from to 7 to 21 ($\times 10^{-3}$) nm $s^{-1}$. The multilayer synthesis proceeds by cycling the gas flow composition between Ar and Ar-25%$N_2$ to produce $N$ number of layer pairs. A 200 W forward power is used to deposit a 0.15-0.16 μm total film thickness $t$. The low

deposition rate combined with the 15-20 sec time interval needed to stabilize the flow rate yields a nominal interfacial width less than 0.3 nm. The multilayer coatings prepared on the Si substrates are vacuum annealed at 450 °C to assess stability. One sample (the *N=20* B/BN coating deposited on Ni/Si) in the as-deposited (t°) condition is also tested for hardness and chemical bonding.

*Microstructure Characterization*

Auger electron spectroscopy coupled with depth profiling indicates the BN coatings have a B to N composition ratio of 4:5.[17] Methods used to examine the microstructure of the multilayer coatings are x-ray diffraction (XRD) in the $\theta/2\theta$ mode and transmission electron microscopy (TEM). Bright field (BF) imaging near the defocus condition along with selected area diffraction (SAD) reveal the growth morphology, multilayer spacing $\lambda$, film texture and crystal structure. The cross-sectioned, *N=20* layer pair B/BN coatings are BF imaged (Fig. 1) along the growth direction (indicated by the arrow). The layers are initially continuous, of equal thickness and conform to the substrate surface. The roughness introduced by the Ni/Si substrate surface (Fig. 1a) results in a more diffuse appearance to the final layers than found for the coating deposited on sapphire (Fig. 1b). Minimum crystallographic information is obtained using XRD and SAD for these B, BN and B/BN films. The high angle $\theta/2\theta$ scans are too shallow, as attributed to a nanometric grain size, for meaningful crystallographic interpretation. The low angle $\theta/2\theta$ scans confirm the $\lambda$ values (as listed in Table I) determined from the sputter deposition conditions and the TEM images. SAD indicates the featureless B coatings are *amorphous* whereas the diffuse ring patterns of the BN and B/BN coatings have interplanar spacings that best fit a disordered hBN phase.[18]

*Hardness Measurement*

A Nanoindenter is used to produce indentation arrays within each film at each of several depths. A Berkovich indenter, i.e. a three-sided pyramid, is used for the hardness measurements. Typically, the indenter is loaded, held at peak load, and then unloaded at a constant rate. Loads are measureable above 0.25 μN and indentation depths to within 0.3 nm. The analysis of nanoindentation load-displacement curves as first developed for bulk homogeneous materials indicate the hardness is equivalent to the indentation load divided by the contact area of the indenter impression.[8] The contact area is proportional to the square of the indentation depth *d*. For hard, stiff materials as well as inhomogeneous systems, modeling of the unloading curve may be beyonds the limitations of linear behavior or a power-law relationship. The assumption

of linear unloading is effected as well as the shape approximation for the indenter tip.[9] Therefore, analysis methods have evolved to better define parameters as true contact area, elastic modulus, and hardness. For example, refinements wherein the indentation load is found to be proportional to $d^2$ provide useful alternatives to finite element methods.[19,20]

The hardness of the B and BN multilayer coating-substrate are determined using the method proposed by Oliver, et al. although there are limitations imposed by analizing these inhomogeneous and hard coatings.[9,21,22] A comparative sampling is provided that can be directly correlated with the multilayer spacing and morphology. A variation in the hardness measured for a single film will occur with different indentation depths.[21] The hardness plots for the B/BN multilayers (Fig. 2) evidence the transition from indenting only the coating to measuring the substrate contribution. A continuous change in hardness is measured as $d/t$ increases to 1, beyond which the curves converge on the substrate hardness of 21GPa for sapphire and 10 GPa for Ni-coated Si. At some critical indentation depth $d_c$, the substrate has influenced the measured film hardness. The coating hardness is determined at $d \leq d_c$ since a variation of hardness with $\lambda$ may exist. Therefore, the hardness measurements at the shallow indentation depths are listed in Table I. The ASTM recommendation to determine coating hardness at $d/t < 0.1$ is followed whenever possible.[23] At the minimum indentation load, the soft films deform readily (noting $d/t > 0.2$) which indicates a substrate contribution to measured hardness. The intrinsic limitation of a minimum resolvable load for nanoindentation prohibits the resolution of a hardness plateau at $d/t < 0.1$ for the very soft (<1 GPa) and thin coatings.

The B/BN hardness (Table I) is found to decrease for $\lambda < 7.5$ nm. The multilayers deposited on sapphire are harder than those on Ni/Si. The relative decrease in multilayer hardness (between substrates for a given $\lambda$) may also be attributed to mixing between the B and BN layers as apparent in the TEM cross-section images (Fig. 1). The layer intermixing is accentuated for the substrate with the rougher surface, i.e. Ni/Si. In fact, the $N=67$ ($\lambda=2.5$ nm) multilayer deposited on sapphire is smoother and harder than the $N=20$ ($\lambda=7.5$ nm) multilayer deposited on Ni/Si. Whereas the hardness of the as-deposited ($N=20$ B/BN)/Ni/Si multilayer sample exceeds the r-o-m value for B/BN, intermixing as a consequence of interdiffusion is also indicated by the significant decrease in hardness as measured after annealing at 450 °C.

*Chemical Bonding*

Near-edge x-ray absorption fine structure (NEXAFS) reveals the distinguishing features of $sp^2$ and $sp^3$ hybridization witihin the boron and nitrogen 1s photoabsorption cross-sections that

are associated with different crystalline phases.[24] The photon energy of monochromatic synchrotron radiation is scanned through the core-level edge while monitoring the electron yield to measure the core-level photoabsorption cross-section. The low-energy, long mean-free-path electron emission dominates the signal yielding a bulk sensitive measurement of the films. The $sp^2$ hybridized, planar bonding that is characteristic of hexagonal BN appears as a narrow and intense transition at 192.0 eV. This $\pi^*$ resonance found in the spectra for the B/BN multilayer films (Fig. 3) is absent in $sp^3$ tetrahedrally bonded materials such as cubic BN which has a single absorption maximum step into $\sigma^*$ continuum states at 194.0 eV.

The sensitivity of NEXAFS to local order provides further detail of bonding defects that exist in the B and BN films.[25,26] The presence of nitrogen void defects in hexagonal BN is found to be indicated by three satellite features above the 192 eV peak in the B 1*s* spectra as found in the spectra of the BN and B/BN films (Fig. 3). Noting that the 192 eV peak is indicative of B-($N_3$) bonding in hexagonal BN, the additional peaks correspond in progression to B-($BN_2$), B-($B_2N$) and elemental boron. A broad peak at 194 eV for the elemental B film (Fig. 3) can be interpreted as correlating with the icosahedral structure and bonding of metallic boron. The spectra of the B/BN multilayers, collected at the same time of the nanoindentation measurements, contain transitions that comprise both the B and BN layers. The BN component of the multilayer shows the $\pi^*$ resonances and the B component evidences the bonding of metallic boron. The intensities of these features are listed in Table I for each curve as determined using a Gaussian fit. The relative intensity of the B component (in comparison to the $\pi^*$ resonances of the BN layer) increases with the measured hardness of the B/BN multilayers. The 450 °C anneal of the (*N=20* B/BN)/Ni/Si sample evidences the metastability of the structure as-deposited at 215 °C. The intensity of the B-($N_3$), B-($BN_2$) and B-($B_2N$) peaks all increase whereas the elemental B peak decreases form the t° condition.

## SUMMARY

Nanoindentation is used to measure the hardness of B, BN and B/BN coatings less than 0.2μm thick. Hard coatings of B which are subject to stress-induced delamination from the substrates are produced by rf sputter deposition from a pure B target. Soft hexagonal BN films are reactively sputter deposited using a B target with a Ar-$N_2$ working gas mixture. Multilayers of B and BN are deposited by modulating the sputter gas composition between Ar and Ar-$N_2$, respectively. Intermixing of layers during deposition as accentuated for substrates with greater surface roughness and intermixing from interdiffusion as a result of annealing both reduce the hardness of the B/BN films. There is no large enhancement of hardness in the B/BN coatings as superlattice effects are not apparent in these multilayer films. However, a 14% increase in hardness above the r-o-m value is found for a 7.5nm layer pair sample. NEXAFS provides a means to assess the chemical bonding within the multilayers that is indicative of the film hardness. The ratio of the $\pi^*$ resonances and elemental boron peak intensities may be developed to predictively determine film hardness.



## ACKNOWLEDGMENTS

We thank the following indivduals and institutes. I. Jimenez lead the x-ray absorption measurements at the Stanford Synchrotron Radiation Laboratory and the Advanced Light Source at Lawrence Berkeley Laboratory. M. Wall performed the transmission electron microscopy at Lawrence Livermore National Laboratory. K. Alexander provided facility use for T.Y. Tsui who performed the nanoindentation measurements while visiting Oak Ridge National Laboratory. This work was supported by the Basic Energy Sciences - Synthesis and Processing Center for Hard Surfaces. This work was performed under the auspices of the United States Dept. of Energy by Lawrence Livermore National Laboratory under contract #W-7405-Eng-48.

## REFERENCES


1. D. Kester, K. Alley, D. Lichtenwainer and R. Davis, J. Vac. Sci. Technol. A12, 3074 (1994).

2. T. Friedmann, et al., J. Appl. Phys. 76, 3088 (1994).

3. T. Wada, and N. Yamashita, J. Vac. Sci. Technol. A10, 515 (1992).

4. N. Tanabe, T. Hayashi and M. Iwaki, Diamond Relat. Mater. 1, 883 (1992).

5. S. Barnett and M. Shinn, Ann. Rev. Mater. Sci. 24, 481 (1994).

6. J. Koehler, Phys. Rev. B 2, 547 (1970).

7. L. Palatnik, A. Il'inskii and N. Sapelkin, Sov. Phys. Sol. Stat. 8, 2016 (1967).

8. M. Doerner and W. Nix, J. Mater. Res. 1, 601 (1986).

9. W. Oliver and G. Pharr, J. Mater. Res. 7, 1564 (1992).

10. U. Helmersson, et al., J. Appl. Phys. 62, 481 (1987).

11. X. Chu, M. Wong, W. Sproul and S. Barnett, Surf. Coatings Technol. 61, 251 (1993).

12. A.F. Jankowski, NanoStruct. Mater. 6, 179 (1995).

13. R.F. Bunshah, R. Nimmagadda, H.J. Doerr, B.A. Movchan, N.I. Grechanuk and G.G. Didkin, Thin Solid Films 112, 227 (1984).

14. D. Makowiecki, A. Jankowski, M. McKernan and R. Foreman, J. Vac. Sci. Technol. A8, 3910 (1990).

15. M. McKernan, D. Makowiecki, P. Ramsey and A. Jankowski, Surf. Coatings Technol. 49, 411 (1991).

16. D. Makowiecki and M. McKernan, *Fabrication of Boron Sputter Targets*, U.S. Patent No. 5,392,981 (February 28, 1995).

17. A. Jankowski, J. Hayes, M. McKernan and D, Makowiecki, Lawrence Livermore National Laboratory UCRL-JC-121985 (1995).

18. A. Jankowski, J. Hayes, M. McKernan and D, Makowiecki, Thin Solid Films, in press (1997).

19. J.L. Loubet, J.M. Georges and J. Meille, in *Microindentation Techniques in Materials Science and Engineering*, p. 72, P.J. Blau and B.R. Lawn (eds.), American Society for Testing and Materials, Philadelphia (1986).

20. S.V. Hainsworth, H.W. Chandler and T.F. Page, J. Mater. Res. 11, 1987 (1996).

21. B.D. Fabes, W.C. Oliver, R.A. McKee and F.J. Walker, J. Mater. Res. 7, 3056 (1992).

22. G.M. Pharr, W.C. Oliver and F.R. Brotzen, J. Mater. Res. 7, 613 (1992).

23. ASTM Standard E 92, *Annual Book of Standards 3.01*, p. 264, American Society for Testing and Materials, Philadelphia (1987).

24. L. Terminello, A. Chaiken, D.A. Lapiano-Smith, G.L. Doll and T. Sato, J. Vac. Sci. Technol. A12, 2462 (1994).

25. I. Jimenez, A. Jankowski, L.J. Terminello, J.A. Carlisle, D.G.J. Sutherland, G.L. Doll, J.V. Mantese, W.M. Tong, D.K. Shuh, and F.J. Himpsel, Appl. Phys. Lett. 68, 2816 (1996)

26. A. Jankowski, Mater. Res. Soc. Symp. Proc. 437, 207 (1996).

**Table 1. B, BN and B/BN multilayer samples**

| (Film)/Substrate | $t$ (μm) | $N$ | $\lambda$ (nm) | $H$ (GPa) | I (B-$N_3$) | I (B-$BN_2$) | I (B-$B_2N$) | I (B) |
|---|---|---|---|---|---|---|---|---|
| (B)/Ni/Si | 0.14 | - | - | 27.0 | 0 | 0 | 0 | 1.00 |
| (B/BN)/Ni/Si @t° | 0.15 | 20 | 7.5 | 15.5 | 0.20 | 0.15 | 0.16 | 0.49 |
| (B/BN)/Sapphire | 0.15 | 20 | 7.5 | 8.5 | 0.15 | 0.29 | 0.26 | 0.29 |
| (B/BN)/Sapphire | 0.17 | 67 | 2.5 | 4.0 | - | - | - | - |
| (B/BN)/Ni/Si | 0.15 | 20 | 7.5 | 1.4 | 0.30 | 0.31 | 0.21 | 0.18 |
| (B/BN)/Ni/Si | 0.17 | 100 | 1.7 | 1.0 | 0.61 | 0.26 | 0.09 | 0.04 |
| (BN)/Ni/Si | 0.26 | - | - | 0.2 | 0.78 | 0.15 | 0.05 | 0.02 |

## Figure Captions

Fig. 1 Bright field images of the 20 layer pair B/BN coatings deposited on the (a) Ni/Si and (b) sapphire substrates, as viewed in cross-section.

Fig. 2 The variation of nanoindentation hardness $H$ with indentation depth normalized to film thickness $(d/t)$ for the B, BN and B/BN coatings.

Fig. 3 The intensity variation of electron yield with photon energy in the B 1*s* spectra for the B, BN and B/BN coatings.

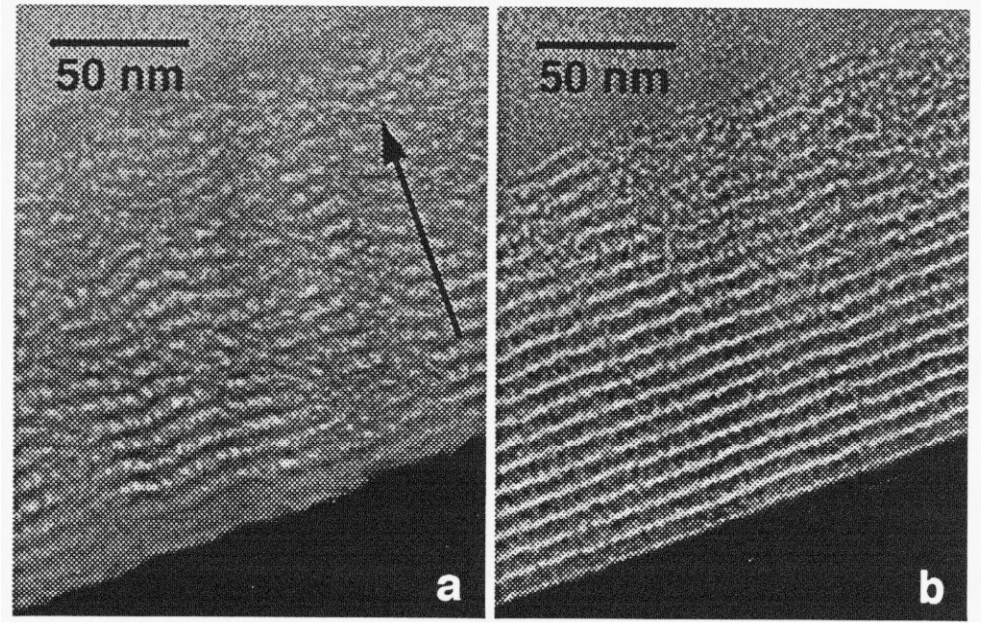
50 nm
a
50 nm
b

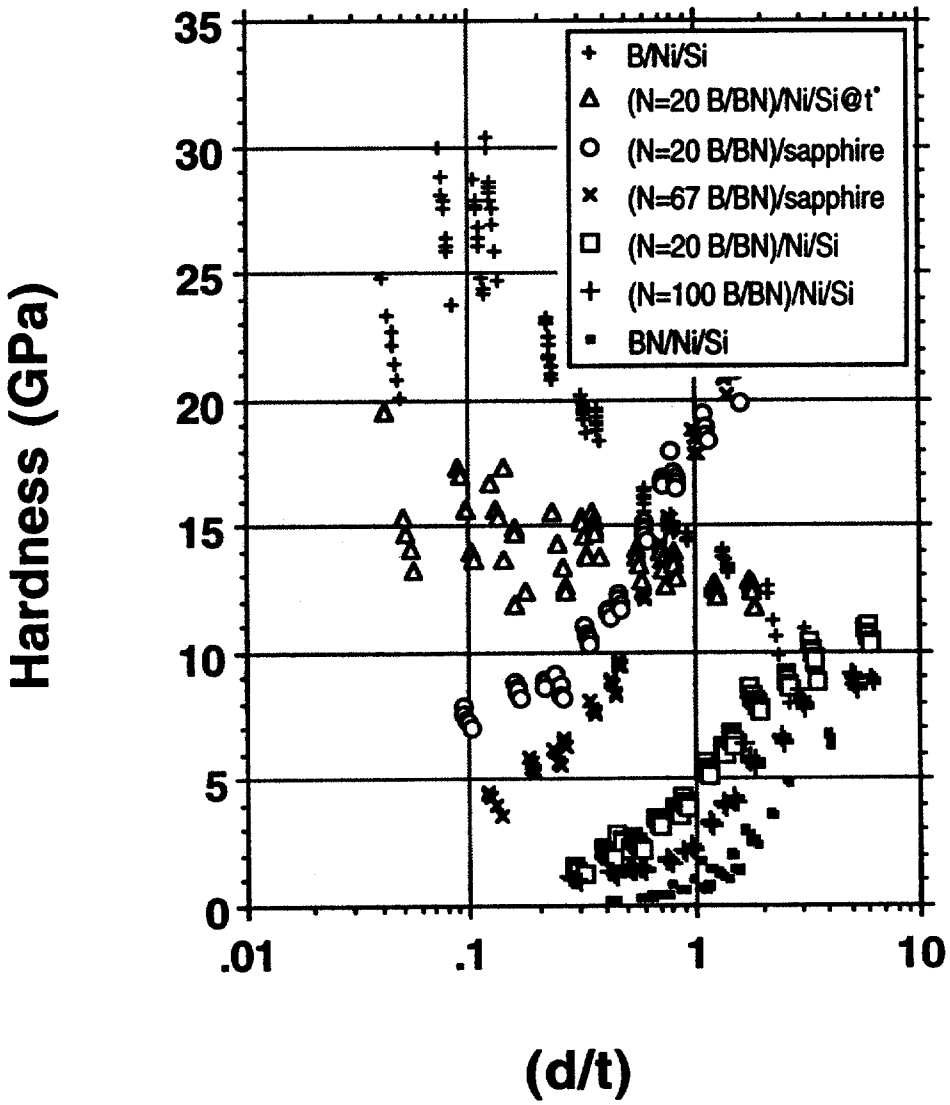
Hardness (GPa)
35
30
25
20
15
10
5
0
.01
.1
1
10
(d/t)
B/Ni/Si
(N=20 B/BN)/Ni/Si@t*
(N=20 B/BN)/sapphire
(N=67 B/BN)/sapphire
(N=20 B/BN)/Ni/Si
(N=100 B/BN)/Ni/Si
BN/Ni/Si

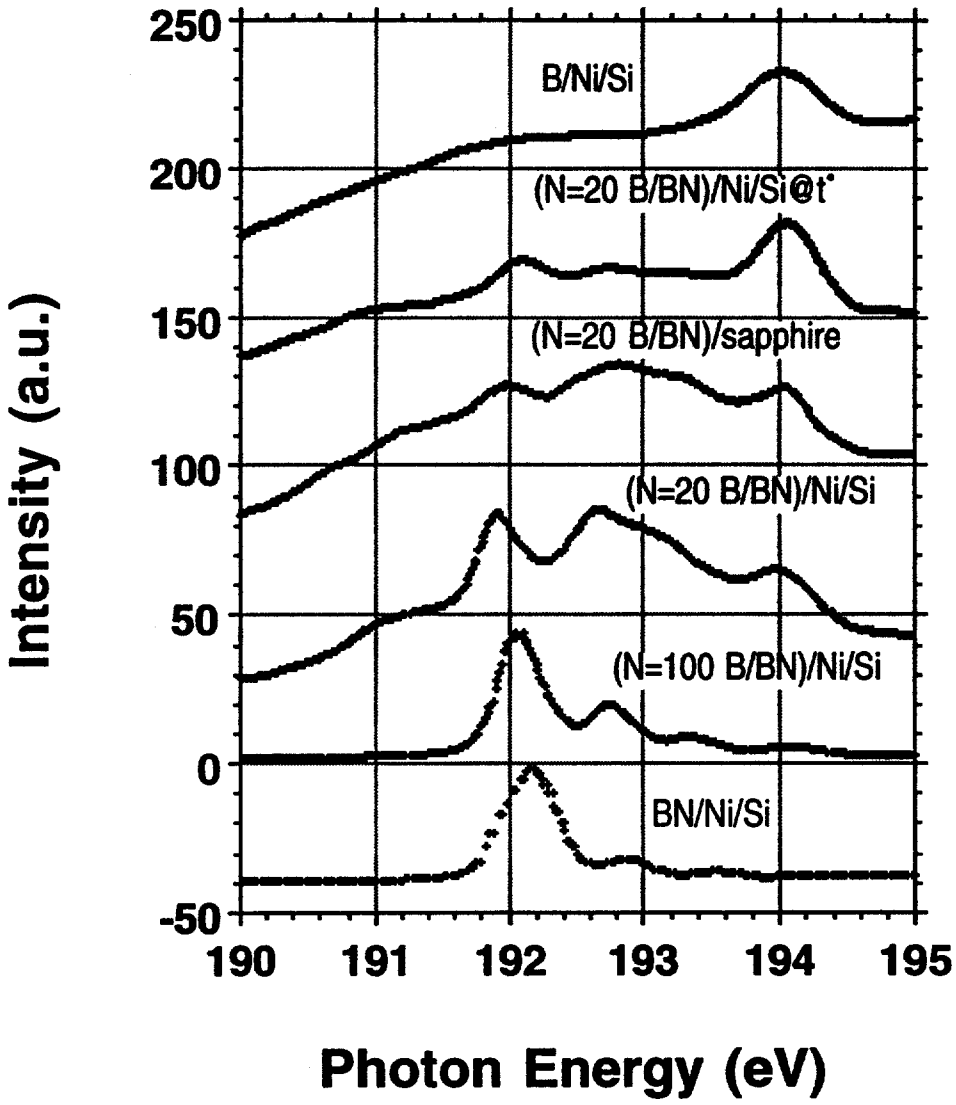
250
200
150
100
50
0
-50
190
191
192
193
194
195
B/Ni/Si
(N=20 B/BN)/Ni/Si@t°
(N=20 B/BN)/sapphire
(N=20 B/BN)/Ni/Si
(N=100 B/BN)/Ni/Si
BN/Ni/Si
Intensity (a.u.)
Photon Energy (eV)

*Technical Information Department* • **Lawrence Livermore National Laboratory**
**University of California • Livermore, California 94551**